2.8 How to Collect Complete Scattering Patterns

Resorting to Debye (cf. p. 1), "*only a continuous scattering pattern can be the funda-
ment of proper reasoning*" the general question must be addressed, how a complete
scattering pattern can be collected. The considerations of this section are based on the
assumption that the scattering pattern is recorded by means of a 2D- or 1D-detector.

2.8.1 Isotropic Scattering

The Limits.   There are a lot of materials whose scattering pattern does not change
if the sample is deliberately rotated in the X-ray beam. Such materials are called
isotropic. For isotropic materials completeness is only a question of the angular range
in which significant scattering information is gathered. The technical limits are de-
fined by the setup, and the fundamental parameter is the distance R between sample
and detector. The smallest accessible scattering angle is given by the size of the beam
stop (cf. p. 37, Fig. 4.1b) which prevents the detector from being damaged by the di-
rect beam. The highest angle with reasonable data is restricted by the extension of
the detector or, worse, by the signal-to-noise (S/N) ratio of the data. If thin samples
are exposed for short time in a weak beam, there is most probably no significant in-
formation in the outer part of the scattering pattern and quantitative data evaluation
is futile. The problem is less severe if a 2D-detector is used. In this case azimuthal
averaging will increase the S/N-ratio in particular at high scattering angles.

How to Arrange the Setup.   In practice, the distance R is long enough, if the
scattering intensity can safely be extrapolated towards zero from the data recorded.
The distance R is short enough, if in the outer part of the scattering pattern, a suf-
ficiently long region with a monotonous background is recorded. One should not
underestimate the need for sufficient recording of background in SAXS and US-
AXS. In order to increase the highest accessible angle, 2D detectors may be placed
in a lateral off-set position with respect to the primary beam.

    If there is no possibility to cover the complete range with one detector, there may
be the possibility to use two detectors which are placed in different distances from
the sample. In the worst case the experiment has to be performed several times with
different setups.

2.8.2 Anisotropic Scattering

Anisotropy is frequently observed in soft materials, but the symmetry of anisotropy
is varying. Fibers and films show, in general, less complex anisotropy than ordinary
or photonic crystals.

2.8.2.1 Single Crystal Anisotropy

Complete scattering patterns of samples with a complex "single-crystal" anisotropy
can only be recorded in a texture setup (Chap. 9, Fig. 9.3). The samples must be
rotated in order to scan the required fraction of reciprocal space.

2.8.2.2 Fiber Symmetry

Definition.   Fiber symmetry is uniaxial or cylindrical symmetry. Revolving the sample about the fiber axis does not change the scattering pattern, but tilting the sample with respect to the fiber axis does.

USAXS and SAXS.   Concerning USAXS and SAXS, the scattering pattern that is recorded on a 2D detector is complete if the principal axis of the sample is set normal to the direction of the incident X-ray beam (primary beam). Completeness is a result of two facts.

1. Fiber symmetry: with the s_3 axis in fiber direction the pattern shows rotational symmetry in the plane (s_1, s_2), thus $I(\mathbf{s}) = I\left(\sqrt{s_1^2 + s_2^2}, s_3\right) = I(s_{12}, s_3)$ is a function of s_3 and of the distance from this axis only.

2. The tangent plane approximation is valid: the curvature of the Ewald sphere is negligible at small scattering angles.

Thus in this favorable case the complete information on nanostructure is recorded in one 2D image. Mathematically the recorded image is a slice

$$\lceil I(\mathbf{s})\rceil_2 (s_1, s_3) \equiv I(s_{12}, s_3). \tag{2.53}$$

It is complete because of fiber symmetry. The 2D Fourier transform of this image is not related to the searched slice, but to a *projection* of the correlation function. In contrast, the sought-after slice in real space

$$\rho^{\star 2}(r_{12}, r_3) = \lceil \rho^{\star 2}(\mathbf{r})\rceil_2 (r_1, r_3)$$
$$= F^2(\{I(\mathbf{s})\}_2 (s_1, s_3)),$$

is the 2D Fourier transform of the projection

$$\{I(\mathbf{s})\}_2 (s_1, s_3) = \int I\left(\sqrt{s_1^2 + s_2^2}, s_3\right) ds_2$$

of the complete intensity from the 3D scattering pattern on the slice formed by the detector plane. Because of completeness it can be computed from the data collected in one 2D scattering pattern.

WAXS and MAXS.   Fiber symmetry means that, even in WAXS and MAXS, the scattering pattern is completely described by a slice in reciprocal space that contains the fiber axis. Nevertheless, for $2\theta > 9°$ the tangent plane approximation is no longer valid and the detector plane is mapped on a spherical surface in reciprocal space.

If we keep the sample's principal axis normal to the primary beam and record a scattering pattern, we can readily map the measured intensities to the plane that we need to know (BUERGER (1942) in ALEXANDER [7], p. 58-62). For this purpose
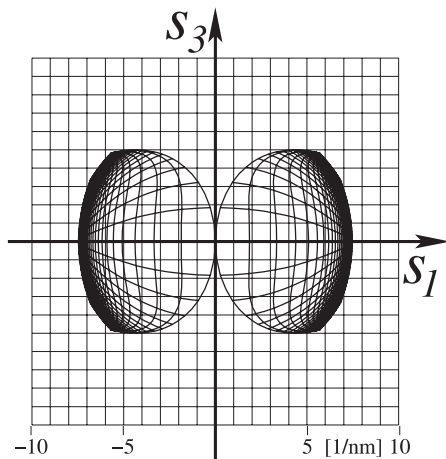
Figure 2.6. WAXS, 2D-detector and fiber symmetry: unwarping of the detector surface to map it on the (s_1, s_3)-slice. Fiber direction is normal to the primary beam. $R = 10$ cm, $\lambda = 0.154$ nm. The warped grid in the sketch is a square grid on the detector (edge length: 3 cm)

we refer to Fig. 2.3 and deduce the out-of-plane component s_2, which is readily established by application of Pythagoras' cathetus theorem[22]. Thereafter we compute the components s_1 and s_3 and receive the mapping equations. The result shows a peculiar deformation (Fig. 2.6). With respect to the slice that contains the complete information, only the area enclosed by solid lines is recorded on the plane detector. There are two blind gusset-shaped areas extending from the center upward and downward along the meridian. Within these areas Bragg peaks may be hidden. Thus the scattering pattern of fibers collected on the 2D detector is not complete if WAXS data are recorded.

It is worth to be noted that not only the position of the pixels, but also their area is modified by the unwarping. Correction of WAXS images thus requires both a translation and a magnification of the intensity proportional to the inverse of the area enclosed by the respective vertices. After the advent of digital computers it became possible to carry out the cumbersome calculus automatically[23], as proposed by FRASER[24] et al. [35].

The solution to access the invisible areas is readily copied from texture analysis: *tilt the sample* by ψ and receive 1 data point on the meridian that corresponds to $s_3 = (2/\lambda) \sin \psi$. The result of the mapping is shown in Fig. 2.7. Thus by recording a series of images taken at different tilt angles of the fiber the blind area can be covered to a sufficient extent. Finally, the remnant blind spots may be covered by means of

---

[22] $(-2s_2/\lambda = s^2$ in the right triangle under THALES' circle whose leg is indicated by a dashed line). The use of the cathetus theorem was suggested by my daughter Agnes.

[23] A corresponding program was presented by RICHARD HILMER (DuPont Inc., Wilmington, USA) at a CCP13 workshop in 1997. The program is property of DuPont.

[24] B. HSIAO and scientists of his group have started to call the algorithm "Fraser correction"
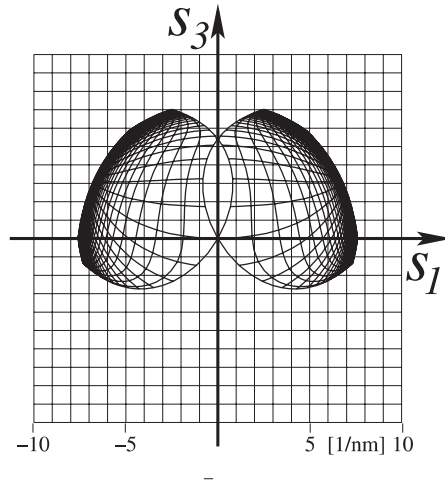
Figure 2.7. WAXS, 2D-detector and fiber symmetry: unwarping of the detector surface to map it on the (s_1, s_3)-slice. Fiber direction is tilted by $\psi = -30°$ with respect to the primary beam. $R = 10$ cm, $\lambda = 0.154$ nm. On the detector the apparent warped grid is a square grid (edge length: 3 cm)

2D extrapolation procedures, e.g., the algorithm based on radial basis functions [36] which is implemented in *pv-wave*® [37].

2.9 Application of Digital Image Processing (DI)

2.9.1 DI and the Analysis of Scattering Patterns

In 1994, when the bottleneck of scattering data analysis was still the poor performance of detectors, RUDOLPH & LANDES were already spotting the bottleneck of our days:

> "Having 2D detection that operates in the cycle time of key experiments means we are then potentially limited by image processing. In other words, as soon as we begin using 2D-detectors to measure patterns, we are forced to use image analysis methods to extract information from the images. With the rapid development of fast detectors, image analysis becomes key to our effective use of this technology."([38], p. 26)

The source code of a set of DI procedures for the processing of scattering patterns written for *pv-wave* is available on the worldwide web (www.chemie.uni-hamburg.de/tmc/stribeck/dl/).

2.9.2 A Scattering Pattern Is a Matrix of Numbers, Not a Photo

Digital image processing starts after we have managed to read the raw scattering image. Each scattering pattern recorded by the detector is a matrix filled with positive integer numbers – the counts in each cell (pixel) of the detector.

For publication such matrices are frequently converted into photos and stored in photo formats (JPEG, GIF, PNG). Such photo files are good for visualization, but no longer good for data evaluation. TIFF is a special case: 8- and 24-bit TIFF files are photos, 16-bit TIFF format is a common storage format for raw scattering patterns[25], but it is not convenient for data evaluation.

Keep your precious raw data. Do not send JPEG- of GIF-encoded color images around for the purpose of "data" evaluation.

2.9.3 How to Utilize DI

The novice at a synchrotron facility should use the pre-evaluation options offered locally at the facility or should resort to the program *FIT2D* [39]. At least pre-evaluation operations like masking of blind areas, background correction, alignment... can be performed this way.

The real business of scattering image processing is more difficult. Because there does not exist a "point-and-click" program, the scientist must write the respective algorithms himself. In order to simplify the work, a dedicated programming system for DI should be chosen. The commercial systems IDL [40] and *pv-wave* [37] offer the key features of DI. Before choosing IDL check if it is now possible to easily write algorithms that work on matrices of varying size. Moreover, a library function for multidimensional extrapolation of data like the radial basis function [36] algorithm of *pv-wave* (RADBE) is essential. If the license fees are a problem, the free ImageJ [41] may be a solution that avoids to start from level-zero programming.

2.9.4 Concepts of DI that Ease the Analysis of Scattering Images

2.9.4.1 The Paradigm: Arithmetics with Matrices

In IDL and *pv-wave* a number, a vector, or a matrix can be handled in the same way. If s is a scattering image, b the parasitic background, and a the actual absorption factor of the sample, then a background correction[26] is carried out writing

```
wave> sc=s-a*b
```

This is not only simple[27], but computes much faster than the common concept of usual programming languages using two encapsulated loops.

---

[25]16-bit-TIFF can be viewed and "processed" by image processing programs (photoshop, gimp,...) the program discards the lower 8 bits in order to make the file an ordinary photo. Ergo: (1) Never overwrite your precious raw data by saving them from a program that was not made for scattering data analysis, (2) What you see in a photo processor is only a fraction of the scattering data.

[26]The example is valid for the most simple case: SAXS or USAXS in normal-transmission geometry.

[27]The same line of code evaluates curves, images or data structures of higher dimensionality (imagine time as an additional coordinate)

If we know that behind the beam stop the intensity is always 50 counts or less, we can discriminate the valid area of our image by defining a ROI mask (i.e., a shape function) (cf. p. 17) by simply writing

```
wave> m=s gt 50
```

which means: generate a matrix m of the same size as s. If a certain pixel in s is greater than (gt) 50, then set the respective pixel in m to 1 (in the logical meaning of "true"; white color; good data). The other pixels are set to 0 (in the boolean meaning of "false"; black color; invalid data).

The result will exhibit the next problem: even some of the valid pixels have not received enough photons to surmount the "blind"-level. The solution for this problem is application of the "closing" operator described at the end of this chapter.

2.9.4.2 Submatrix Ranking Operators

Submatrix ranking operators are belonging to the class of image-space operators (HABERÄCKER [42]) in contrast to Fourier-space operators.

Practical Problems that are Solved by the Operations. Consider you have defined a mask and it turns out that pixels close to the edges of the blind areas did not receive the true intensity due to a *penumbra* effect. How do you peel off the penumbra region easily?

Consider you have forgotten to switch on "multi-read"[28] with your CCD detector and the raw data are full of cosmic-ray spikes. How do you remove them without spoiling the image?

Definition: Submatrix. We choose a deliberate pixel from our scattering image. The pixel and its neighboring pixels are the submatrix. For the example we choose a submatrix size of 3×3 elements. There is scattering intensity in each pixel, e.g.

$$53\ 68\ 47$$
$$57\ 67\ 52\,.$$
$$57\ 64\ 43$$

Definition: Ranking. Now let us rank these values by sorting them in increasing order

$$\mathbf{43}\ 47\ 52\ 53\ \mathbf{57}\ 57\ 64\ 67\ \mathbf{68}\,.$$

2.9.4.3 Primitive Operators: Erode, Median, and Dilate

Based on the ranked list DI defines three primitive submatrix ranking operators. They determine, which value is put in the center of the submatrix:

---

[28]cf. Sect. 4.2.5.2

erode: Take the leftmost (smallest) value from the list (i.e. 43),

median: Take the value from the center of the list (i.e. 57),

dilate: Take the rightmost (biggest) value from the list (i.e. 68).

Erode applied to a mask peels off a layer from every "white" island in the mask. Dilate does (almost) the inverse: if erode has not managed to delete a white island completely, it is almost restored. The median operator reduces noise in the image without broadening the peaks. The operator is frequently addressed "median filter".

In practice, the abovementioned penumbra problem is solved by eroding the mask. Choose the size of the submatrix according to the width of the penumbra or try out by peeling-off thin layers repetitively. Then multiply the scattering image by the eroded mask and thus mark the penumbra region as "invalid".

In similar manner, spikes in the image from cosmic rays are extinguished by simple application of the median filter with a small submatrix size (3 or 5).

2.9.4.4 Combined Operators: Opening & Closing

Particularly useful are two operators that are combined from two primitive submatrix ranking operators.

Opening (also: ouverture) is erosion followed by dilation. The ouverture removes tiny "white" islands in the matrix if their area is smaller than half the area of the chosen submatrix.

Closing (also: fermeture) is dilation followed by erosion. The operator closes isolated "black holes".

Thus in order to fill small black holes in a mask, the closing operator will do automatically what otherwise would have to be done by hand[29].

From their definition the DI operators are easily implemented. Nevertheless, this implementation work is unnecessary if IDL or *pv-wave* are used, where the respective operators are simply picked from the rich library.

In fact, digital image processing systems have much more to offer – in image space, where the alignment and centering of scattering images is carried out with ease, but also in Fourier space where the predefined library functions are easily adapted to the needs of scattering pattern analysis on the fundament of scattering theory. Respective information is collected from textbooks on the field of DI and from the manuals of IDL or *pv-wave*.

---

[29]Probably by painting with the "mouse"